BOUNDARY MATCHING FOR THE INTERIOR EXTERIOR HELMHOLTZ EQUATION

MATT MAHONEY

Abstract. We study the Interior Exterior Helmholtz Problem and examine the convergence of a numerical technique based on boundary integral equations.

1. The Helmholtz Equation

The Helmholtz equation $(\triangle + k^2)f = 0$ governs the steady state solutions of the wave equation in a homogeneous (k constant) medium. We wish to explore solutions of the 2-D Helmholtz equation where in some bounded domain $\Omega \subseteq \mathbb{R}^2$ the wavenumber k_1 is different from the wavenumber k_2 in the ambient space. This models situations such as light in vacuum being scattered by a lens or, analogously, light in a medium with an air pocket in it. We call this the Interior Exterior Helmholtz Problem.

To begin setting up notation, let $v(x)$ denote the solution inside Ω, i.e.

$$(\triangle + k_1^2)v = 0. \tag{1.1}$$

Likewise, let $u(x)$ denote the solution outside Ω, i.e.

$$(\triangle + k_2^2)u = 0. \tag{1.2}$$

In order to specify this solution uniquely we must impose boundary conditions on each u and v at the interface between the two media. The relevant boundary conditions in this case are continuity,

$$u(x) = v(x), \tag{1.3}$$

and differentiability,

$$u_n(x) = v_n(x), \tag{1.4}$$

for all $x \in \partial\Omega$. Here the subscript n denotes the derivative of the function in the outward normal direction.

The fundamental solution, $\Phi(x, y)$,of the Helmholtz equation is $H_0^{(1)}(k|x - y|)$, the zeroth Hankel function of the first kind. We will stick with standard terminology and call the fundamental solution a monopole and the derivatives of the fundamental solution dipoles.

2. Boundary Integral Methods

It is well known that both interior and exterior solutions to the Helmholtz equation can be written as integrals of monopole and dipole densities on the boundary of Ω. This result is standard and follows from Green's Representation Formula.

Disclaimer: In order not to recapitulate all of the theory that was taught in Math 116 in the winter of 2006, the relevant notation will be taken verbatim from the course notes and copied here for bookkeeping purposes. Provided you are reading this paper, it is (almost certainly) the case that you are either a student from the course, the professor of the course, or you found this paper on a website next to the course notes. In any event, the prerequisite theory should be accessible to you.

Integral Operators: Let $\sigma, \tau : \partial\Omega \to \mathbb{C}$ and $x \notin \partial\Omega$

$$(S\sigma)(x) := \int_{\partial\Omega} \Phi(x,y)\sigma(y)ds_y \tag{2.1}$$

$$(D\tau)(x) := \int_{\partial\Omega} \frac{\partial\Phi(x,y)}{\partial n_y}\tau(y)ds_y \tag{2.2}$$

$$(D^T\sigma)(x)) = \int_{\partial\Omega} \frac{\partial\Phi(x,y)}{\partial n_x}\sigma(y)ds_y \tag{2.3}$$

$$(T\tau)(x) = \int_{\partial\Omega} \frac{\partial^2\Phi(x,y)}{\partial n_x \partial n_y}\tau(y)ds_y \tag{2.4}$$

Jump Relations: For $f(x) = (S\sigma)(x)$, $g(x) = (D\tau)(x)$ and $x \in \partial\Omega$

$$f(x) = (S\sigma)(x) \tag{2.5}$$

$$f_n^{\pm} = (D^T\sigma)(x) \mp \frac{1}{2}\sigma(x) \tag{2.6}$$

$$g^{\pm}(x) = (D\tau)(x) \pm \frac{1}{2}\tau(x) \tag{2.7}$$

$$g_n = (T\tau)(x) \tag{2.8}$$

Boundary integral methods reduce the problem of solving the Helmholtz equation to constructing the appropriate monopole and dipole densities so that these densities, when fed into the above integral operators, produce the desired solution. The rest of this paper will be concerned with how to do this for the IEHP.

3. Solving the Interior Exterior Helmholtz Problem

The method we will use to solve the IEHE will be to represent the scattered field inside and outside $\partial\Omega$ with layer potentials (i.e. as integrals of monopole and dipole densities along $\partial\Omega$). The field incident on our object will be a plane wave $u^{inc} = e^{i\vec{k}\cdot x}$ outside Ω and $v^{inc} = 0$ inside Ω. Although the fields inside and outside Ω satisfy the HE in their respective domains, the boundary conditions are not met

at the interface. The goal is to construct scattered fields u^s and v^s inside and outside respectively so that for all $x \in \partial\Omega$ we have

$$u^{inc}(x) + u^s(x) = v^{inc}(x) + v^s(x) \tag{3.1}$$

and

$$u_n^{inc}(x) + u^s(x) = v_n^{inc}(x) + v^s(x). \tag{3.2}$$

In addition to simply being a restatement of the boundary conditions, these equations intimate the method for finding the scattered fields. Rearranging equations (3.1) and (3.2) we get

$$u^s(x) - v^s(x) = -(u^{inc}(x) - v^{inc}(x)) \tag{3.3}$$

$$u_n^s(x) - v_n^s(x) = -(u_n^{inc}(x) - v_n^{inc}(x)) \tag{3.4}$$

for $x \in \partial\Omega$.

We can begin by setting the incident fields as arbitrary solutions of the Helmholtz equation inside and outside Ω. In our case, we used a plane wave for the outside incident field and the zero solution for the inside. It is this choice that explains the terminology incident and scattered. One does, however, need an explicit representation for the incident fields since they will be evaluated in the course of the numerical computations.

We then represent the scattered fields inside and outside using monopole and dipole densities on the boundary. Recall that the fundamental solution $\Phi(x, y)$ is wavenumber dependent and correspondingly so are the S, D, and T operators. We will use subscripts to make this distinction. The superscript s will be suppressed from now on unless context dictates its' necessity (to partially save us from what might still be a notational nightmare).

$$v(x) = (S_1\sigma_1)(x) + (D_1\tau_1)(x) \tag{3.5}$$

$$u(x) = (S_2\sigma_2)(x) + (D_2\tau_2)(x) \tag{3.6}$$

We can now use the jump relations for these representations to rewrite equations (3.3) and (3.4) as

$$(S_2\sigma_2)(x)+(D_2\tau_2)(x)+\frac{1}{2}\tau_2(x)-(S_1\sigma_1)(x)-(D_1\tau_1)(x)+\frac{1}{2}\tau_1(x) = -(u^{inc}(x)-v^{inc}(x)) \tag{3.7}$$

$$(D_2^T\sigma_2)(x)-\frac{1}{2}\sigma_2(x)+(T_2\tau_2)(x)-(D_1^T\sigma_1)(x)-\frac{1}{2}\sigma_1(x)-(T_1\tau_1)(x) = -(u_n^{inc}(x)-v_n^{inc}(x)). \tag{3.8}$$

It is here that we need to make a technical point. Both of the operators S and T have singular kernels. In the case of T, the kernel is hypersingular. We can fix

this problem by setting $\sigma = \sigma_1 = \sigma_2$ and $\tau = \tau_1 = \tau_2$. This allows us to write the above system as

$$(S_2 - S_1)(\sigma)(x) + (D_2 - D_1)(\tau)(x) + \tau(x) = -(u^{inc}(x) - v^{inc}(x)) \tag{3.9}$$

$$(D_2^T - D_1^T)(\sigma)(x) - \sigma(x) + (T_2 - T_1)(\tau)(x) = -(u_n^{inc}(x) - v_n^{inc}(x)). \tag{3.10}$$

The benefit of this maneuver is that it pits the singularities of each operator against the other. In particular, we know that kernel of S_2 is asymptotic to $\ln(|x - y|)$, whereas the kernel of $-S_2$ is asymptotic to $-\ln(|x - y|)$. These singularities mutually cancel so that the kernel of $S_2 - S_1$ is continuous. Similar, although more in depth, arguments can be made about the kernel of $T_2 - T_1$ showing that it is too well-behaved along the diagonal.

What we are left with now is a coupled system of linear integral equations. To solve them numerically we replace the integrals with quadrature approximations to obtain a matrix equation. The solution of this matrix equation yields a discrete approximation of the functions σ and τ which can used to construct the scattered field.

4. Numerical Experiments

The follow numerical experiments used the interior of the ellipse $\frac{x^2}{4} + \frac{y^2}{25} = 1$ as the domain Ω. This particular shape was chosen for a number of reasons, the most technical of which being that $\partial\Omega$ is smoothly parameterizable. This makes the use of equal weight quadrature efficient. In addition, the hope was that an ellipse was enough of a lenslike shape that the numerical simulations would show the incident plane wave being focused.

To test the convergence of the method the first test was to set $k_1 = k_2$ and see if the incident wave simply traveled through the lens. Note that this is not a vacuous test because the interior solution was initialized at zero. Figure 1 shows plots of a slice through the approximate solution at $y = 0$ for various numbers of quadrature points. The interface between the two media is at $x = \pm 2$. As is evident, for large enough numbers of quadrature points the solution does begin to match on either side of the interface. (I'm sorry I was unable to get $LaTe\chi$ to label the figures properly.)

Since in this case the analytical solution is known, we are able to make explicit error calculations. Figure 2 is a plot of the log of the error at the point $(1.8, 0)$ as a a function of the number of quadrature points. Note that there is a definite slope indicating exponential convergence.

For the next series of simulations, we took $k_1 = 1.5$ and $k_2 = 1$.

Figure 3 is a density plot of the total solution through an elliptical lens with boundary satisfying $x^2 + \frac{y^2}{9} = 1$ and with $k_1 = 1.5$ and $k_2 = 1$. Figure 4 is a 3D plot of the same simulation.

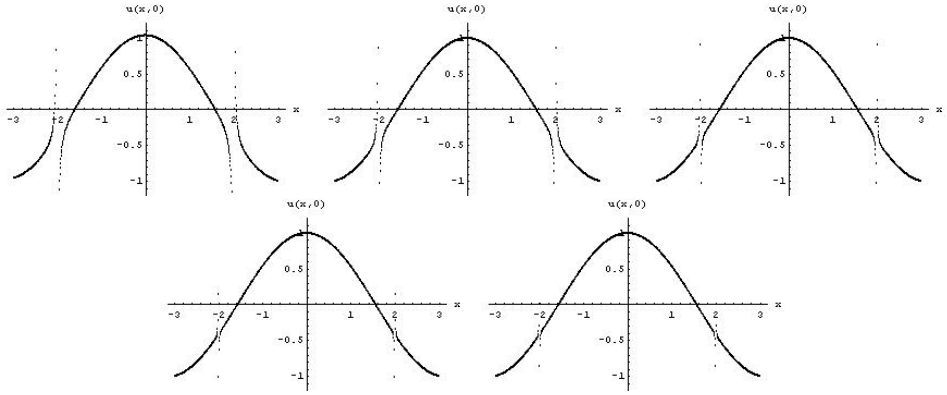

FIGURE 1. Slices at y=0 for 20, 40, 80, 160, and 200 quadrature points.

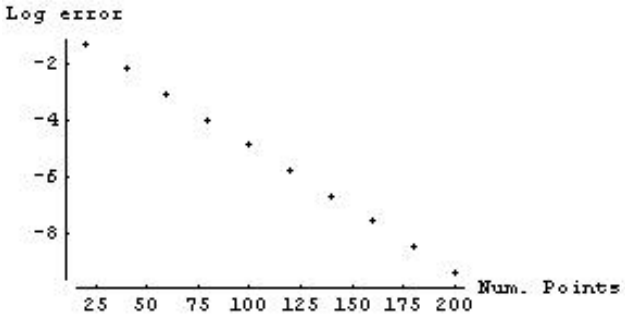

FIGURE 2. Log of error as a function of the number of quadrature points used in the approximation.

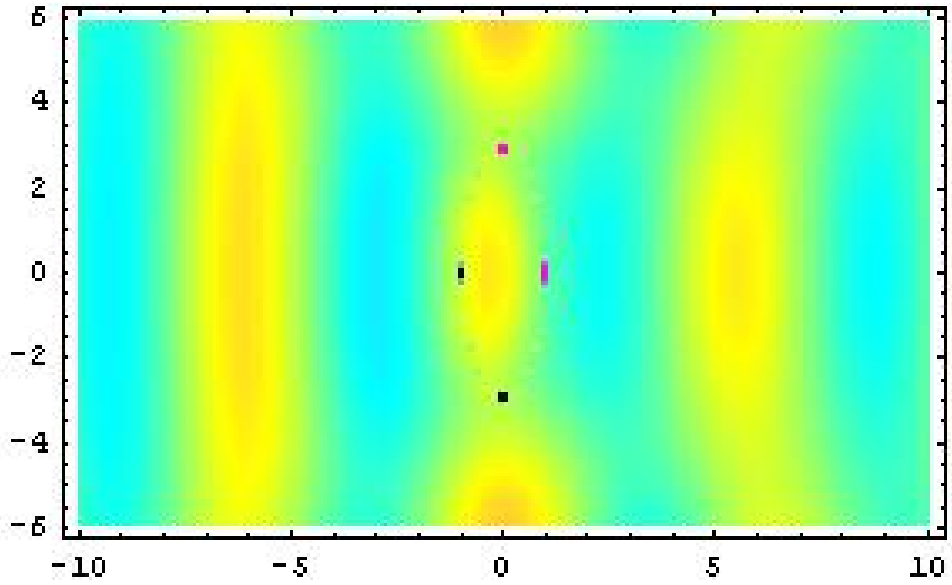

FIGURE 3. Density plot of the field in elliptical lens with boundary $x^2 + \frac{y^2}{9} = 1$. (Please pardon the fact that I have not demarcated the boundary of the ellipse. *Mathematica*® acting up again!)

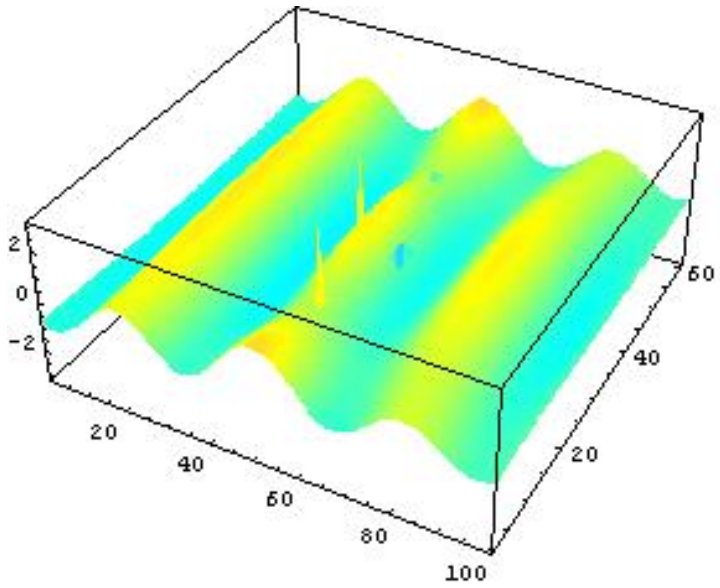

FIGURE 4. 3D plot of the field in elliptical lens with boundary $x^2 + \frac{y^2}{9} = 1$. (Please pardon the fact that I have not demarcated the boundary of the ellipse. *Mathematica*® acting up again!)